

AD-A161 286

A VORTEX MODEL FOR WALL FLAME HEIGHT(U) FEDERAL
AVIATION ADMINISTRATION TECHNICAL CENTER ATLANTIC CITY
NJ T I EKLUND SEP 85 DOT/FAR/CT-85/17

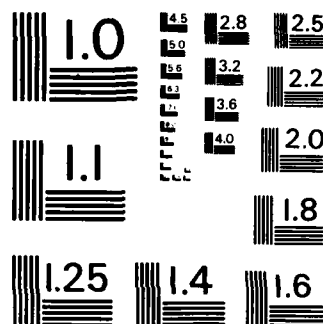
1/1

UNCLASSIFIED

F/G 21/2

NL





MICROCOPY RESOLUTION TEST CHART
NATIONAL BUREAU OF STANDARDS-1963-A

12

DOT/FAA/CT-85/17

FAA Technical Center
Atlantic City Airport
N.J. 08405

A Vortex Model for Wall Flame Height

AD-A161 286

Thor I. Eklund

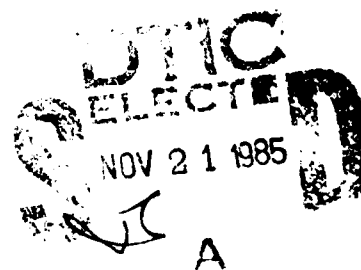
September 1985

This document is available to the U.S. public
through the National Technical Information
Service, Springfield, Virginia 22161.

DTIC FILE COPY



U.S. Department of Transportation
Federal Aviation Administration



85 11 15 004

NOTICE

This document is disseminated under the sponsorship of the Department of Transportation in the interest of information exchange. The United States Government assumes no liability for the contents or use thereof.

The United States Government does not endorse products or manufacturers. Trade or manufacturer's names appear herein solely because they are considered essential to the object of this report.

Technical Report Documentation Page

1. Report No. DOT /FAA/CT-85/17	2. Government Accession No. AD A161 256	3. Recipient's Catalog No.	
4. Title and Subtitle A VORTEX MODEL FOR WALL FLAME HEIGHT		5. Report Date September 1985	
		6. Performing Organization Code ACT-350	
7. Author(s) Thor I. Eklund		8. Performing Organization Report No.	
		10. Work Unit No. (TRAIS)	
9. Performing Organization Name and Address Federal Aviation Administration Technical Center Atlantic City Airport, New Jersey 08405		11. Contract or Grant No.	
		13. Type of Report and Period Covered Final	
12. Sponsoring Agency Name and Address U.S. Department of Transportation Federal Aviation Administration Technical Center Atlantic City Airport, New Jersey 08405		14. Sponsoring Agency Code	
		15. Supplementary Notes	
16. Abstract <p>A two-dimensional vortex model is developed to describe flames on burning walls. The flame is considered a region of intense vorticity generation and is modeled by an equivalent vortex filament. Flame height is predicted by matching the induced air-flow to stoichiometric requirements based on wall mass loss rate or energy release rate. The vortex model predicts the same two-thirds power law relationship that has been determined from other approaches. The quantitative predicted height is within the published limits of experimental certainty.</p>			
17. Key words Fire Vorticity Flame Height Heat Release Rate		18. Distribution Statement Document is available to the U.S. public through the National Technical Information Service, Springfield, Virginia 22161	
19. Security Classif. (of this report) Unclassified	20. Security Classif. (of this page) Unclassified	21. No. of Pages	22. Price

TABLE OF CONTENTS

	Page
EXECUTIVE SUMMARY	v
INTRODUCTION	1
Purpose	1
Background	1
Objective	1
ANALYSIS	2
DISCUSSION	4
CONCLUSIONS	6
REFERENCES	6

SEARCHED ☒ **SERIALIZED** ☒

INDEXED ☒ **FILED** ☒

MAY 1968
FBI - NEW YORK

A-1



LIST OF ILLUSTRATIONS

Figure		Page
1	Idealized Wall Flame	7
2	Circulation Integration Path	8
3	Buss Bar Magnetic Field	9
4	Flame Vortex Representation	10

EXECUTIVE SUMMARY

Vorticity theory has been successfully used to theoretically predict and explain lift forces on wings, ground effects during aircraft takeoff and landing, and minimum separation standards for avoiding trailing vortices from large aircraft. Although aircraft wings are relatively large areas of vorticity generation, in many applications these regions can be treated as vortex filaments. While aircraft vorticity generation is ultimately caused by frictional effects, vorticity in fires is often caused by pressure and buoyancy forces. If a fire plume is viewed as a region of vorticity production somewhat analogous to a lifting surface, the possibility of approximating flow effects by a vortex filament arises as a reasonable approach.

In this analysis, two classical vortex equations (Bjerknes theorem and the Biot-Savart law) are used to characterize the vorticity produced by a burning wall. The vorticity, which is dispersed throughout the flame, is idealized by a single vortex filament located in the upper half of the visible flame. By employing a mirror vortex element behind the wall, the air induced into the flame can be calculated. This influx of air, coupled with the stoichiometric requirements for complete combustion of the fuel evolved from the wall, leads to an analytic relationship for the size of the flame based on either the mass loss rate of the wall or the energy release rate.

The final relationship agrees well with theoretical and experimental results recently published. The use of vortices to describe flow fields caused by fires offers a powerful method to analyze specific fire problems that might be extremely difficult to attack by other techniques.

INTRODUCTION

Purpose.

The purpose of the effort is the development of a simply derived relationship between material burning rate and flame height on walls.

Background.

Fire growth in aircraft cabins involves material ignition, burning rates, and flame spread rates along with attendant effects on the gas phase environment within the enclosure. The fire plumes from burning materials are additionally significant because of their potential for directing heat at nearby or adjacent materials and causing fire involvement of additional fire load. For instance, if the visible fire plume of a burning seat impinged on the ceiling, flame spread on the ceiling surface could start, provided that necessary ignition criteria were met. Similarly, if a section of wall were burning, the height of the fire plume would dictate how much material and possibly what type materials were exposed to direct flame. The height of wall flames has direct implications for upward fire spread and implicit bearing on material selection and spacing. These implications have been addressed through analysis and experiment (references 1, 2, 3, and 4). The analyses have been done with dimensional analysis as well as integral methods employing boundary layer type equations. These approaches involve use of an entrainment coefficient to account for the introduction of enough oxygen to support combustion of the flammable volatiles from the pyrolysis zone of the burning wall. An example of the type relationship developed from such approaches (reference 1) is

$$y_f = 4.2 \left(\frac{\dot{Q}}{C_p T_o \rho_o \sqrt{g}} \right)^{2/3} \quad (1)$$

where \dot{Q} is the energy release rate, C_p is the specific heat of air, T_o and ρ_o are the ambient gas temperature and density, respectively, g is the gravitational constant, and y_f is the flame height. Similar equations involve a different coefficient from 4.2, radiation correction factors, as well as different arrays of terms used to factor the heat release rate. The striking common denominator to the experimental data and theoretical predictions for turbulent wall fires is that the flame height is proportional to the two-thirds power of the heat release rate term.

While the utility of entrainment coefficients is well established for turbulent jets, wakes, and plumes; there is another approach that could be employed in analysis of a burning wall. The alternate approach involves viewing the flame as a region of vorticity generation. Once the vorticity generation is modeled, the air required for combustion will be provided by induction rather than by a turbulent entrainment mechanism.

Objective.

The objective of this analysis is the use of classical vorticity theorems to establish the relationship between flame height and burning rate for wall fires.

ANALYSIS

Vorticity is a defined quantity describing rotational movements in fluids. While vorticity is most often associated with viscous forces in boundary layers, it can also be produced by pressure and density gradients in fluids. While vorticity itself is defined as the curl of the velocity vector, an additional measure of vorticity is the fluid dynamic circulation around a closed loop in a fluid. This is the line integral of the vector dot product of velocity and the loop vector element. The starting point for this development is Bjerknes Theorem (reference 5) which is stated as follows:

$$\frac{d\Gamma}{dt} = - \int_A \nabla \left(\frac{1}{\rho} \right) \times (\nabla p) \, dA \quad (2)$$

where Γ is the circulation, and the right-hand side represents a surface integral of the vector cross product of density and pressure gradients. In a wall flame, the pressure gradient is vertical and the density gradient is horizontal. Figure 1 shows a schematic of an idealized wall flame and the corresponding pressure and density gradients. To the extent that these gradients are perpendicular, the vector cross product will give a unity value to the trigonometric sine term. For the wall flame, equation 2 can be restated as:

$$\frac{d}{dt} \left[\oint \vec{v} \cdot d\vec{l} \right] = \int_0^y \int_0^\delta \frac{\partial \left(\frac{1}{\rho} \right)}{\partial x} \frac{\partial p}{\partial y} \, dx \, dy \quad (3)$$

where δ is the width of the integration region and y is a portion of the flame height. A basic assumption now made is that the flame is defined by some average visible colored region and that the temperature of this region is 1800° F throughout. In this way, the density terms in equation 3 can be redefined as temperature terms through the perfect gas law. Figure 2 shows an integration path for equation 3. The x-axis integral can be approximated by the following term for the density gradient:

$$\frac{R}{p\delta} (T_F - T_A)$$

where T_F is the flame temperature and T_A is the ambient temperature (equivalent to T_0 in equation 1).

Integrating over the distance δ the term comes to

$$\frac{R}{p} (T_F - T_A)$$

The pressure gradient term is that caused by gravity or $\rho_A g$ which can be written as gp/RT_A . Thus, the integral of equation 3 on the right-hand side is

$$\frac{T_F - T_A}{T_A} g y \quad (4)$$

Assuming a steady flame, the left-hand side of equation 3 can be redefined as:

$$V \frac{d}{dy} \int V \, dy = v^2$$

Thus equation 3 simplifies to:

$$v^2 = \frac{T_F - T_A}{T_A} g y \quad (5)$$

This is because shrinking δ to zero removes the line integrals in the x - direction, and outside the flame the y velocity vector is approximated as zero. Thus, Bjerknes theorem leads to the relationship that the velocity of gases in the flame are proportional to the square root of the distance from the base of the flame. Since the circulation around a loop is identical to the total vorticity of the area bounded by the loop, equation 5 shows that the vorticity increases higher into the flame.

At this point, it is convenient to amass this dispersed vorticity into a single vortex filament. The vertical location of the vortex will be taken at the point where half the vorticity of the flame is above it. Since the circulation integral goes like the integral of the square root of y, the location of the vortex, y_v will be taken when

$$y_v^{3/2} = \frac{(y_f)^{3/2}}{2} \quad (6)$$

or when y_f is 1.59 y_v . Going back to equation 5 and integrating the velocity through the entire flame, the total vortex strength at y_v can be taken as

$$\Gamma = \frac{2}{3} \sqrt{\frac{(T_F - T_A)}{T_A}} g y_f^{3/2} \quad (7)$$

This vortex will be located at a close but unspecified distance, δ_v , from the burning wall.

At this point, the model of the vortex and its strength does not provide any relationship to the burning rate of the wall. To develop this relation, two further relationships are needed. First, it will be assumed that the flame tip occurs when enough oxygen has been brought into the flame to combust the burning wall volatiles at a stoichiometric ratio. Second, the vortex strength must be used to find the air induced into the flame. The first of these can be stated as:

$$\dot{m}_A = \left(\frac{a}{f}\right)_s \dot{m}_f \quad (8)$$

The second requires a measure of the total flow induced by the vortex.

Figure 3 shows the type magnetic field produced between two buss bars. The magnetic field lines are the analog to the velocity streamlines in vortex theory. From the illustration in this case, all inflow ends at the midsection of the buss bar. From there, outflow begins. In this vein, the gas flow between the vortex location and the wall will be determined as shown in figure 4. That is,

$$\dot{m}_A = \rho_F V_v \delta_v \quad (9)$$

Figure 4 also shows a mirror vortex on the other side of the wall. This vortex is used to create a flow field preventing velocity components normal to the wall. To find the flow field induced by these vortices of opposite sense, the Biot Savart law is used as described in reference 6.

$$\vec{v} = \frac{\Gamma}{4\pi} \int \frac{d\vec{l} \times \vec{r}}{r^3} \quad (10)$$

The induced velocity from each filament at the wall will consequently be

$$v_1 = \frac{\Gamma}{2\pi \delta_v} \quad (11)$$

If this is taken as the velocity induced in the flame at this point, then the volumetric flow will be given as

$$v_I \delta_v = \frac{I'}{\pi} \quad (12)$$

Employing equation 7 and 12 and multiplying by flame density,

$$\rho_F v_I \delta_v = \rho_F \frac{2}{3\pi} \sqrt{\frac{(T_F - T_A) g}{T_A}} y_F^{3/2} \quad (13)$$

Using equation 8, equation 13 becomes

$$\left(\frac{a}{f}\right)_s \dot{m}_f = \rho_F \frac{2}{3\pi} \sqrt{\frac{(T_F - T_A) g}{T_A}} y_F^{3/2} \quad (14)$$

Equation 14 shows that the flame height is proportional to the burning rate (or energy release rate) to the two-thirds power as shown in equation 1.

DISCUSSION

The form taken by the results of a vorticity analysis differs from the forms yielded in other analyses, primarily from the fact that the specific heat and the entrainment coefficient do not appear at all in the vorticity analysis. For comparison with equation 1, which has the parameters used for data analysis in this area, some reworking of equation 14 is necessary.

Rearranging terms results in

$$y_f = \left[\left(\frac{a}{f}\right)_s \frac{\dot{m}_f}{\rho_F} \frac{3\pi}{2} \sqrt{\frac{T_A}{(T_F - T_A) g}} \right]^{2/3} \quad (15)$$

Assuming that the mass loss rate, \dot{m}_f , can be converted to energy release rate, \dot{E} , by multiplication by some heat of combustion, ΔH_c ,

$$\dot{E} = \dot{m}_f \Delta H_c \quad (16)$$

then equation 15 can be written as

$$y_f = \left[\left(\frac{a}{f}\right)_s \frac{\dot{E}}{\rho_A \Delta H_c} \frac{3\pi}{2} \sqrt{\frac{T_F^2}{T_A (T_F - T_A) g}} \right]^{2/3} \quad (17)$$

This can be converted to a form like equation 1 by multiplying numerator and denominator by the missing terms to get

$$y_f = \left[\left(\frac{a}{f}\right)_s \frac{3\pi}{2\Delta H_c} \sqrt{\frac{T_F^2}{T_A (T_F - T_A)}} (C_p T_A) \right]^{2/3} \left[\frac{\dot{E}}{C_p T_A \rho_A \sqrt{g}} \right]^{2/3} \quad (18)$$

To compare equation 18 with equation 1, the first term on the right hand side has to be evaluated. The parameters used are as follows:

$$\begin{aligned}\left(\frac{a}{f}\right)_s &= 10 \\ \Delta H_c &= 10 \text{ k J/g} \\ C_p &= .24 \text{ cal/g } ^\circ\text{C} \\ T_F &= 1800^\circ \text{ F} \\ T_A &= 70^\circ \text{ F}\end{aligned}$$

Using these numbers,

$$y_f = 5.0 \left[\frac{\dot{E}}{C_p T_A \rho_A \sqrt{g}} \right]^{2/3} \quad (19)$$

Given the uncertainties in flame height measurements as well as the different assumptions used in a vortex approach, the close agreement between equation 19 and equation 1 is remarkable. In experiments by Hasemi quoted in reference 3, the coefficient would be 2.9 for the height of continuous flame and 6.1 for the upper most flame tips.

The common finding between this vorticity approach and previous studies is that \dot{E}/\sqrt{g} to the two-thirds power or \dot{m}/\sqrt{g} to the two-thirds power is the most important pair of terms for flame height correlations. However, the development of the vortex model raises questions about the importance of other factors in accurately modeling flame height. The vortex model induces only enough air to combust the pyrolyzing material while the entrainment coefficient used in reference 3 would involve entraining between 3 and 6.6 times stoichiometric air into the flame. This issue could be resolved by experiment. The entrainment theories incorporate the specific heat as a primary parameter while the vortex theory circumvents this requirement. The reason C_p appears in the right-hand side of equation 19 is that its inverse is included in the factor 5.

The vorticity model clearly demonstrates the wall flame as a region of intense vorticity generation. Although this vorticity was rolled into a single filament for calculational purposes, the actual flame vorticity is of necessity dispersed and disorganized. In actual flames, the vorticity cannot roll into a row of discrete vortices because the wall condition would place mirror vortices directly opposite to them. It is known that the only stable situation involves staggered vortices. This vortex instability can have some influence on wall flame tip oscillation.

While the vortex model does conveniently explain wall flame height and provide insight into flame stability, the major weakness of the model is that it does not explicitly give a flame thickness. Thus, without further boundary layer type analyses, the vortex model's utility is limited insofar as determining heat transfer to the wall for flame spread rate prediction.

CONCLUSIONS

Development of a vortex model to predict wall flame height leads to the following conclusions:

1. The wall flame height is proportional to either the mass injection rate or the energy release rate to the two-thirds power as predicted by other theories and found in experiment.
2. The coefficient to the standard heat release rate array of terms predicted by the vortex model is well within experimental uncertainty.
3. An imaginary vortex filament can satisfactorily represent the dispersed vorticity of the flame for calculations.
4. The velocity increases with square root of height as the flame is traversed vertically.
5. The vorticity of the flame causes air for combustion to be added by an induction mechanism.

REFERENCES

1. Delichatsios, M. A., Modeling of Aircraft Cabin Fires, NBS-GCR-84-473, September 1984.
2. Quintiere, J. G., et al., The Role of Aircraft Panel Materials in Cabin Fires and Their Properties, DOT/FAA/CT-84/30, June 1985.
3. Quintiere, J. G., Harkleroad, M., and Hasemi, U., Wall Flames and Implications for upward Flame Spread, AIAA 23rd Aerospace Sciences Meeting, Paper AIAA-85-0456, January 1985.
4. Alpert, R. L., Pressure Modeling of Fire Growth on Char-Forming and Laminated Materials, DOT/FAA/CT-83/24, June 1983.
5. Prandtl, L., and Tietjens, O. G., Fundamentals of Hydro and Aero Mechanics, New York: Dover Publications, 1957.
6. Robertson, Aerodynamics in Theory and Application, Englewood Cliffs, N.J.: Prentice-Hall, Inc., 1965.

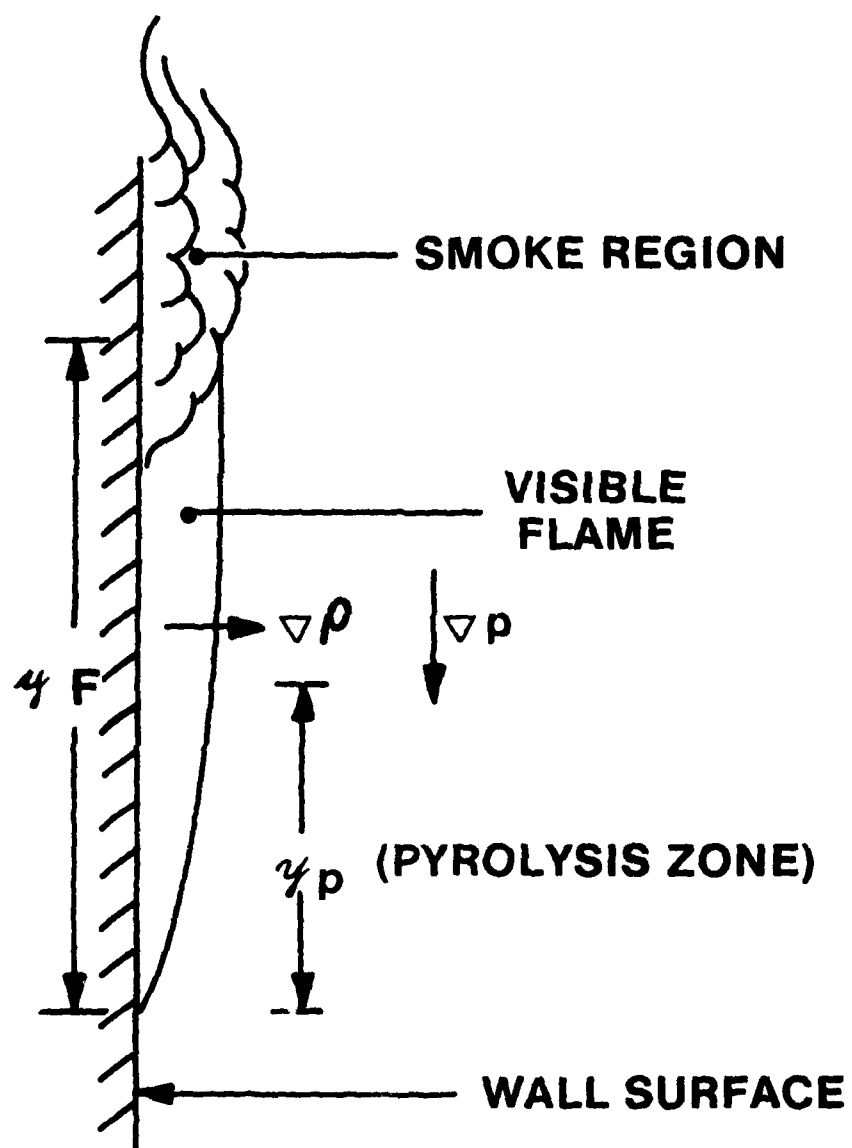


FIGURE 1. IDEALIZED WALL FLAME

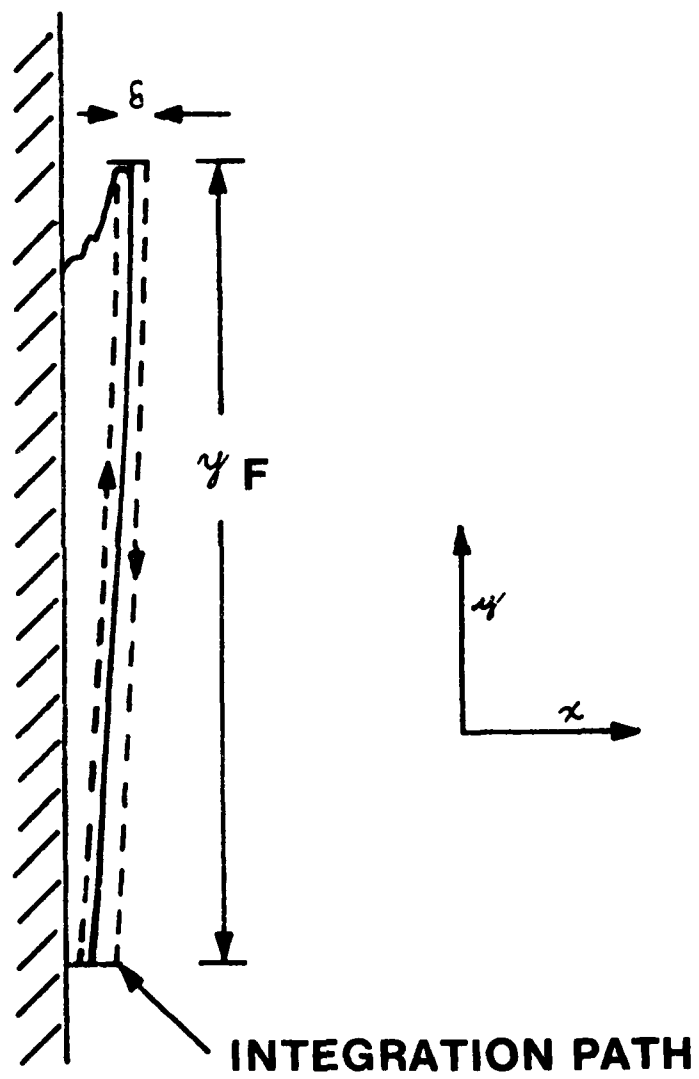


FIGURE 2. CIRCULATION INTEGRATION PATH

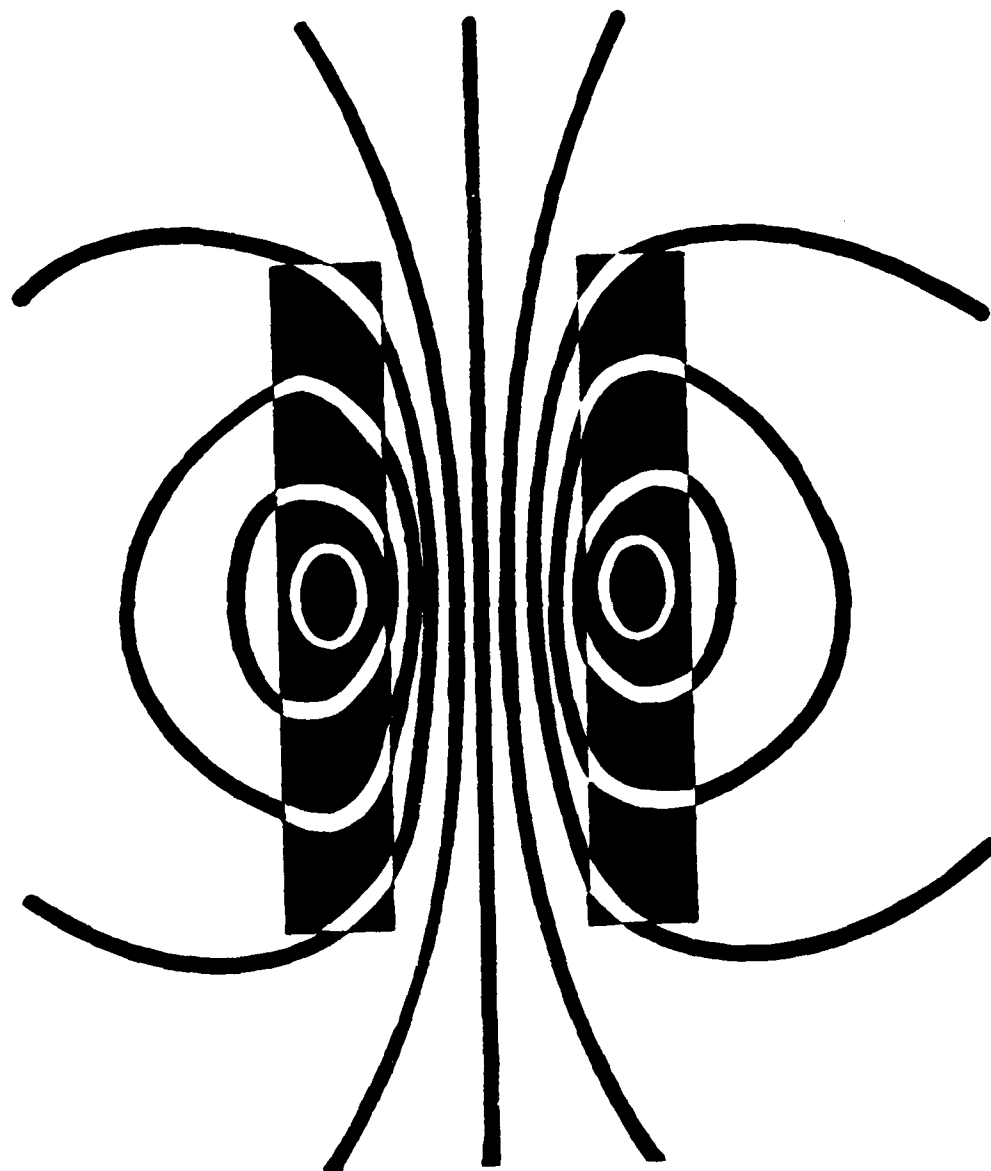


FIGURE 3. BUSS BAR MAGNETIC FIELD

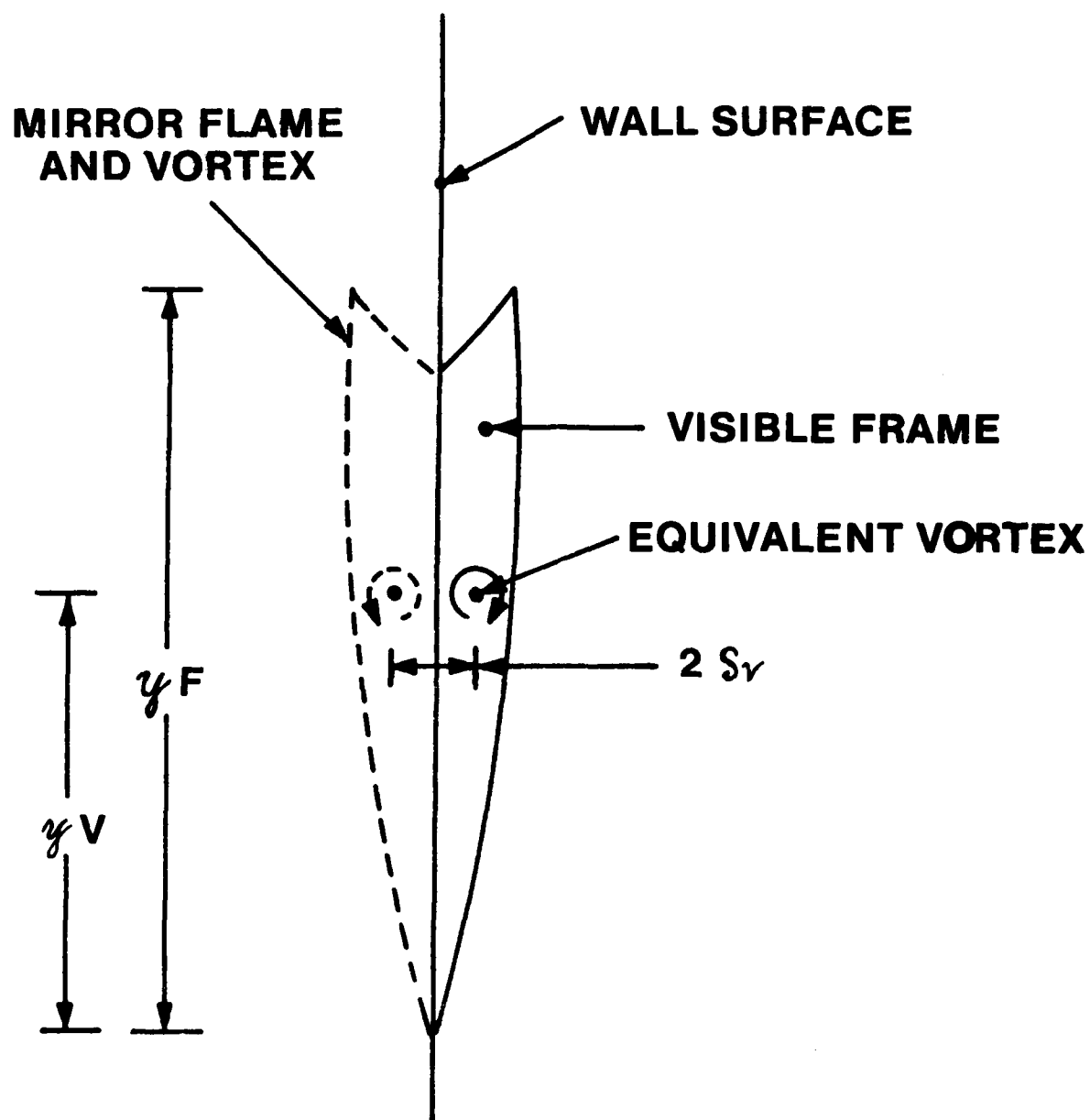


FIGURE 4. FLAME VORTEX REPRESENTATION

END

FILMED

1-86

DTIC